PERIODICO di MINERALOGIA
established in 1930

Dipartimento di Scienze della Terra
Sapienza Università di Roma

An International Journal of
Mineralogy, Crystallography, Geochemistry,
Ore Deposits, Petrology, Volcanology
and applied topics on Environment, Archaeometry and Cultural Heritage

Geochemistry of Paleozoic Dadaş Shales from the Foreland of Southeastern Turkey, Bismil, Diyarbakır

Dicle Bal Akkoca * and Ümit Işık

Fırat University, Faculty of Engineering, Department of Geological Engineering, 23100, Elazığ, Turkey

ARTICLE INFO

Submitted: December 2016
Accepted: June 2018
Available on line: September 2018

* Corresponding author:
dbal@firat.edu.tr

DOI: 10.2451/2018PM683

How to cite this article:
Bal Akkoca D. and Işık U. (2018)
Period. Mineral. 87, 207-225

ABSTRACT

The Early Silurian-Early Devonian Dadaş Shales are composed of sandstone-banded, carbonate-interbedded shales and organic material-rich shales. The sediment geochemistry, along with mineralogical investigations of two core samples from Dadaş Shales have been carried out in order to understand their provenance, paleoweathering, paleoredox, paleoclimate and tectonic conditions. Samples are mainly composed of feldspars, quartz, clay minerals, calcite and dolomite. Chemical index of alteration (CIA) indices reflects medium weathering. Th/Sc and low Zr/Sc ratios suggest no (or at least minor) sediment recycling and sorting. The C-values of Dadaş Shales show mainly moist climatic conditions prevailed during Early Silurian-Early Devonian. Ni/Co vs V/Cr, U/Th, Cu/Zn, Ce/Ce anomaly yielded oxic depositional conditions. The provenance discrimination diagram show magmatic and partly sedimentary provenance for Dadaş Shale. Th/U, Rb/Sr, La/Ni, Cr/Th, La/Yb, Eu/Eu*, $(La/Yb)_N$, $(Gd/Yb)_N$ ratios and the chondrite-normalized REE patterns of the Dadaş Shales are similar to that of Post Archaean Australian Shale (PAAS), and those of Upper Continental Crust (UCC). Source rock composition vary from felsic to neutral and higher values of Sc/Th, Cr/Th, Co/Th in Dadaş Shales with respect to sands from silicic rocks may show the presence of relatively higher proportion of basic material in their source. The provenance discrimination diagram, La/Th versus Hf diagram also show mixed felsic/basic source fields. According to new discriminant-function multi-dimensional diagram for low-silica clastic sediments, Dadaş Shales are plotted within the continental rift field.

Keywords: Paleozoic; Dadaş Shales; provenance; climatic conditions; southeastern Turkey.

INTRODUCTION

The chemical composition of shales is controlled by factors such as source area, weathering, and grain-size sorting during transport, sedimentation, diagenesis and metamorphism (McLennan et al., 1993; Cullers and Podkovyrov, 2000). The distribution of some elements, such as rare earth elements (REEs), Y, Sc, Th, Zr, Hf, Cr, Co and their elemental ratios can be used as geochemical tracers due to their immobility during weathering and transportation processes (Cullers, 2000; Nyakairu and Koeberl, 2001), Geochemical studies have been carried out on shales in order to better understand their provenance characteristics, weathering processes, paleoclimate, paleoredox conditions and tectonic settings (Bauluz et al., 2000; Lee, 2002; Khanehbad et al., 2012; Tawfik et al., 2017).

Paleozoic sedimentary rock sequences which have been partly or slightly affected from the Alpine orogenesis in Turkey retain significant records on source rock, tectonic setting and paleogeographic evolution. In addition the Lower Paleozoic depositional history, tectonics and geological evolution of these units are not yet fully

understood, due to scarcity of detailed biostratigraphical and geochemical studies. The Paleozoic part of rocks in southern Turkey is called Arabian Platform or southeast Anatolian Autochthon. Paleozoic Dadaş Shales under investigation are Upper Paleozoic shales exposing around the Bismil-Diyarbakır area in southeast Anatolia. Investigations in the Dadaş Shales have been continued since 2011 by the Turkish National Petroleum Company (TPAO) and several international companies. Geological and organic geochemical characteristics of the sedimentary rocks of southeastern Turkey were investigated by Bozdoğan et al. (1987), Perinçek et al. (1991), Kavak and Toprak (2013), Özdemir and Ünlügenç (2013). Bozkaya et al., (2009) determined new mineralogical findings on diagenesis-metamorphism of Paleozoic-Lower Mesozoic rocks in the Diyarbakır-Hazro region. Tolluoğlu and Sümer (1995) set forth Early Paleozoic aged monzogranitic magmatic rocks in southeast Anatolia. Göncüoğlu and Turhan (1984) and Kozlu and Göncüoğlu (1997) studied the Early Paleozoic evolution of southeastern Turkey and suggested that Silurian sediments representing the Dadaş Shales are interlayered with sandstones that contain lithic fragments of felsic rocks. On the basis of mineralogical, petrographical and field observations, the Dadaş Shales have been interpreted as a Silurian rift basin. However, the above mentioned studies are not supported by geochemical data. Therefore, the geochemical signatures of Dadaş Shales might provide strong evidences of the source rocks, changing depositional environment, weathering conditions, climatic conditions and tectonics. The aim of this work is to constrain the provenance, depositional history and tectonic setting of Dadaş sediments. Geochemical characterization were made on the cutting samples from the Derindere and Çeltikli cores which were drilled through the Dadas Formation by the Turkish Petroleum Corporation (TPAO) in the years of 2008-2009. These samples were studied for major, trace and rare earth element geochemistry. We explored how successfully geochemical evidences can be used as proxies during the Paleozoic time. It will be evaluated the composition of the core sediments, weathering intensity, sediment provenance, depositional environment and tectonic setting. Petrological and geochemical studies are very limited in southeastern Turkey. Given that such Paleozoic sequences are very common within Southeast Anatolian Autochthon; this pioneering study with special emphasis on geochemical parameters will provide in a regional sense primary data for future investigations on Paleozoic rocks.

MATERIAL AND METHODS

Geological setting

The cores are located in the east and northwestern of Bismil, Diyarbakır, southeastern Turkey (Lat. Derindere: 37 º52’59”.32 N, 40º50’12”.66 E, Çeltikli: 37º50’17”.64 N, 40º53’23”.32 E). The cores cut the Paleozoic units at the bottom hole. A stratigraphic columnar section of Paleozoic units of southeastern Turkey is illustrated in Figure 1. The distribution of Paleozoic units in the southern Turkey is given in Figure 2a. The oldest rocks (Mid-Upper Cambrian) are named as the Derik Group and the upper part of the group is composed of shale, marl, siltstone, sandstone and quartzite of the Sosink Formation. Ordovician time is represented by two formations: Lower Ordovician Seydisehir Formation composed of sandstone, siltstone and quartzite intercalations and Mid-Upper Ordovician Bedinan Formation is composed of silty shales interbedded with sandstone layers. The Bedinan Formation has regressive characteristics that form a shallowing upward sequence. Its lower shale member represents a deeper marine environment (Iztan, 2004), while the upper member is mainly composed of siltstone and sandstones

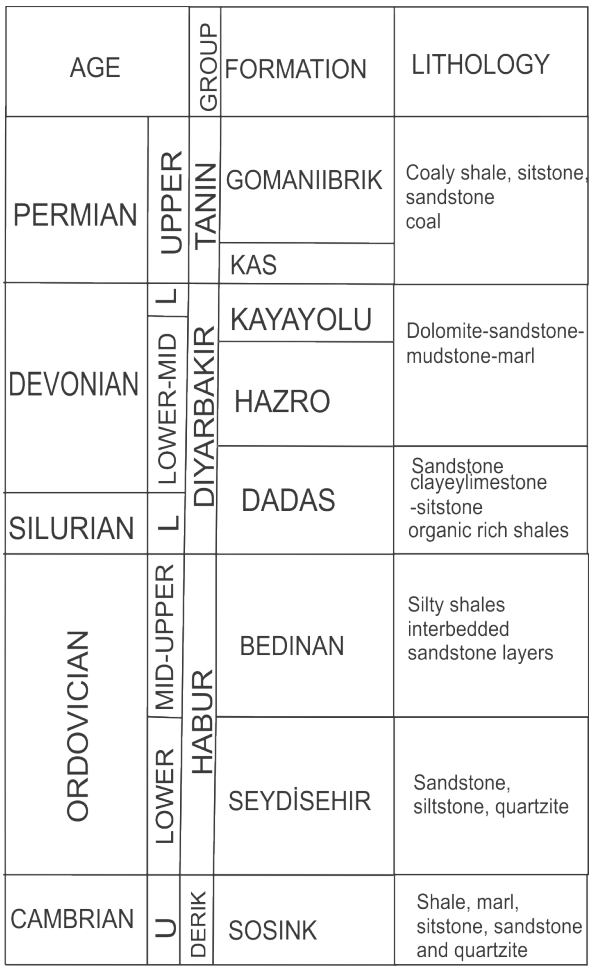

Figure 1. Stratigraphic columnar section of Paleozoic units in southeastern Turkey (Aydemir, 2012).

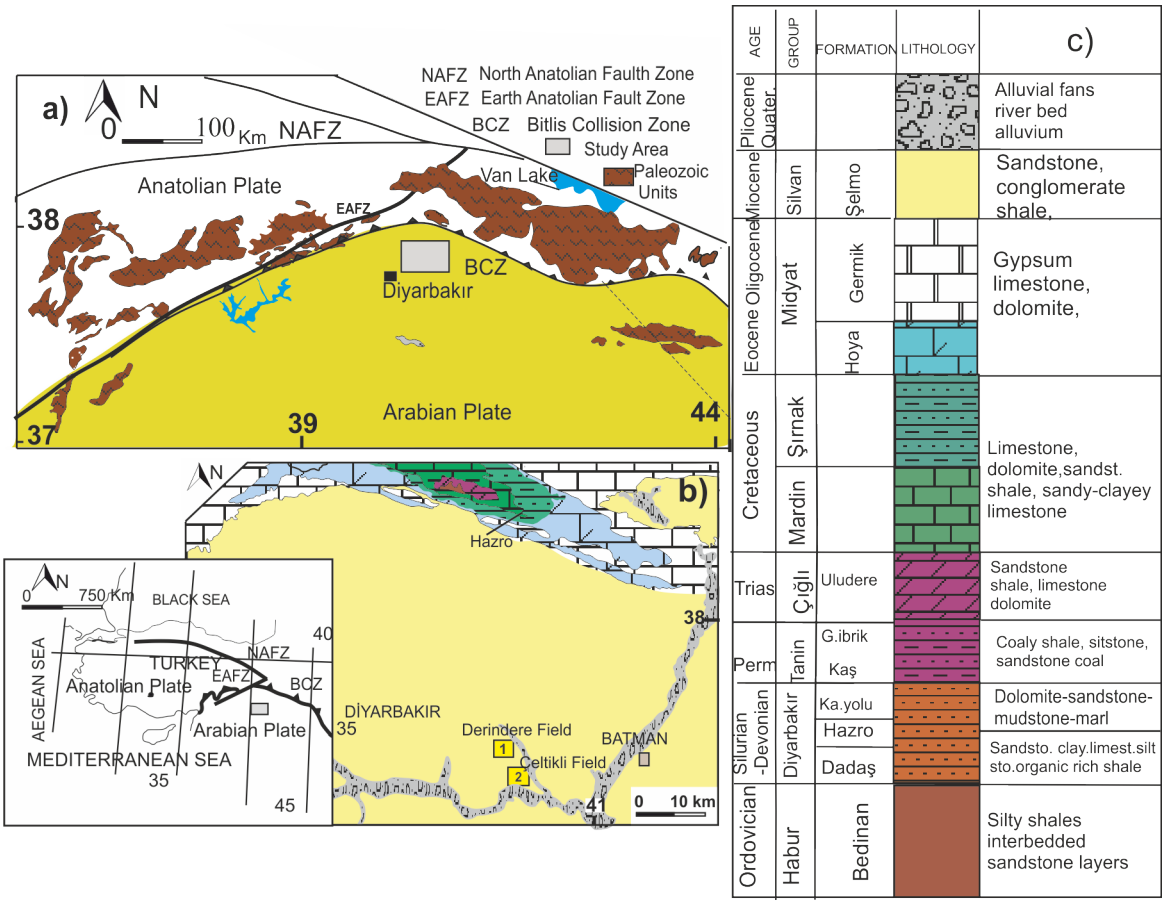

Figure 2. a) The distributions of the Paleozoic units at the southern Turkey, b) Geological map of the study area showing the locations of Derindere core and Çeltikli core. Simplified from 1/500.000 scale geological map of Turkey, published by the General Directorate of Mineral Research and Exploration of Turkey (MTA 2002), c) The general stratigraphic section of the study area (Bozdoğan et al., 1987).

deposited in the shallow marine environment. The Bedinan Formation is unconformably overlain by the Early Silurian-Early Devonian Dadas Formation. They change upward to Devonian Hazro-Kayayolu and Upper Permian Tanin Group (Figure 2b-c). The Dadas Formation under investigation is composed of three members: The basal unit of the formation, Dadas-I Member is composed of organic-rich shales alternated with carbonates, Dadas-II is composed of marine, carbonated shales and clayey limestones. The member becomes siltier in the upper part. The Dadas-III on top consists of shales alternated with sand facies deposited in a shallow marine environment. The Dadas Formation is observed as a transgressive/regressive sequence throughout the northern Arabian Platform (Aydemir, 2012). The map of drilling area is shown in Figure 2b. In the map area, Miocene Şelmo Formation overlies the Early Silurian-Early Devonian Dadaş Shales and other units. Other units exposing in the area are Devonian Hazro, Upper Permian Tanin Group, Lower Triassic Çığlı Group, Cretaceous Mardin-Şırnak Group, Eocene-Oligocene Midyat Group, Pliocene-Quaternary recent alluvial fans and river bed alluvium deposits (Figure 2c).

Hazro-Kayayolu Formation is represented by gray-green colored dolomitic marls with pinkish colored stiff, sandy dolomite intercalations, brown-claret colored sandstone, gray-green mudstones, white laminated cream-colored sandstones, brown patchy green marl and green to brown colored marls. The Tanin Group overlying the upper parts of the Hazro Formation contains coaly shale, siltstone, sandstones and also coal occurrences. Çığlı Group is represented by a sandstone-shale succession, sandy-clayey limestone, dolomite and limestones. Mardin-Şırnak Group includes cherty limestone, dolomite, limestone, sandstone, and mudstone. Midyat Group is composed of gypsum, limestone, dolomite whilst the overlying Şelmo Formation is made up with sandstone, conglomerate and shale (Stolle et al., 2011).

Sampling and analytical methods

Samples were collected from the 190-m long Derindere

and 160-m long Celtikli cores. Units cut in both cores are lithologically similar and gradually change to each other. The resistivity and density of Derindere and Çeltikli core are shown in Figure 3. Gamma-gamma (density-resistivity) logs also respond well to lithology. The decrease in resistivity and density reflects a different compaction trend in these levels (Figure 3).

At the upper most of two cores, thin sandy layer is present. Limonite-bearing dark and light green brownish muds with silty clay layer intercalations are present at depth of 2880-2920 m in the Derindere core and at depth of 2630-2650 m in the Çeltikli core. Greenish-gray shales are dominant at depth of 2920-3000 m in the Derindere core and at depth of 2650-2730 m in the Çeltikli core. White-gray colored carbonaceous shales, and rare organic matter are found at depth of 3000-3030 m in the Derindere core and at depth of 2730-2760 m in the Çeltikli core. Higher organic matter contents are shown at depth of 3030-3070 m and 2760-2790 m in the Derindere core and Çeltikli core, respectively (Figure 3).

Bulk mineralogy of twenty samples was determined by X-ray powder diffraction (XRD) (Rigaku DMAXIII), using Ni-filtered CuKα at 15 kV-40 mÅ instrumental settings. In whole-rock analysis, feldspar was identified using reflections at 3.16 Å, dolomite at 2.92 Å, calcite at 3.03 Å, quartz at 3.33.The whole-rock mineral percentages were determined following the technique described by Gündoğdu (1982) after Brindley (1980). All samples were analyzed as random mounts. The characteristic peak intensities (I) of minerals were normalized to that of the (104) reflection of dolomite. In other words, a K factor for each mineral (including clays with peaks between 19 and 20° theta) was determined as K = I dolomite/I mineral in a 1:1 dolomite mineral mixture by weight. Percentages of the minerals were calculated from the following equation: % of mineral a=100xKaxIa/[(KaxIa+KbxIb)+…KnxIn)] (Ka: peak intensity of minerals; Ia: coefficient of minerals). Accordingly, the areas of the air dried 3.04 Å peak (Ka) were multiplied by 0.74 (Ia) to yield calcite, the area of the 3.34 Å peak (Kb) was multiplied by 0.34 (Ib) to obtain quartz, the 3.20 Å peak areas were multiplied by 1.62 to estimate feldspar, the 4.48 Å peak areas (Kn) were

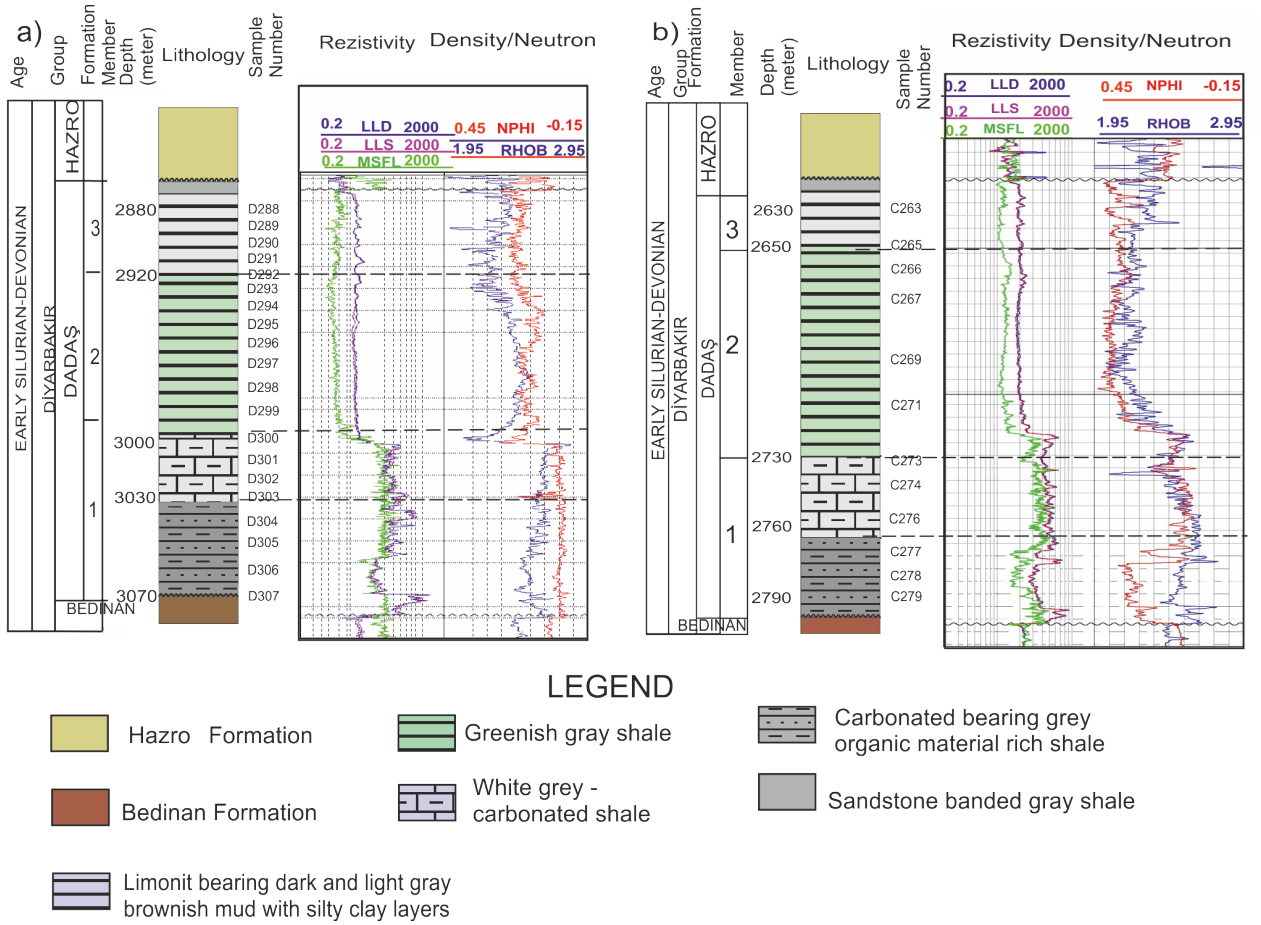

Figure 3. Columnar section and sample horizons of a) Derindere, b) Celtikli cores from Dadaş Shales.

multiplied by 14.63 (In) to yield clay mineral contents. The relative error of this method is less than 15%.

The geochemical analyses of 32 representative samples were carried out at ACME Analytical Laboratories Ltd. (Canada) using ICP-AES and MS for the determination of major, trace elements and rare-earth elements (REE). Furthermore, Total carbon (TC) and sulfur (TS) contents were measured at ACME Analytical Laboratories Ltd. (Canada) by using Leco analysis. Loss on ignition was determined by weight difference after ignition at 1000 °C. In order to determine the relation between the elements and organic material, total organic carbon (TOC) analysis was performed. TOC (%) analysis was conducted at Geochemistry Laboratories of Turkish Petroleum Corporation (TPAO) by the pyrolysis method using the Rock-Eval 6 analyzer. Correlation coefficients were calculated from the data set of the geochemical analyses. Accordingly, the significance level is α=0.05 r value of less than 0.30 is small effect or weak correlation, values of 0.50 and above represent a large effect strong correlation (McCarroll, 2016).

RESULTS

Mineralogy

The results of X-ray diffraction analysis on whole-rock samples from the Derindere and Çeltikli are listed in Table 1. The average abundances of clay minerals, calcite, dolomite, feldspar and quartz are 67.4 wt%, 8.3 wt%, 9.7 wt%, 7.1 wt% and 7.5 wt% in the Derindere core and 59.2 wt %, 9.4 wt (%), 11 wt%, 11.5 wt% and 8.9 wt% in the Çeltikli core, respectively (Figure 4 a,b; Table 1). Calcite content increases between the depths of 3000 and 3020 m in Derindere samples and from 2730 to 2760 m in the Çeltikli samples which are consistent with lithologies in both cores.

All the samples exhibit high proportions of clay minerals and high values of the Mudrock Maturity Index [MMI=100xphyllosilicates/(phyllosilicates+quartz+feldspars)] (Bathia, 1985).

Geochemistry

Major and trace element geochemistry

Major and trace element concentrations, average (ẋ), standard deviations (Std) and variation coefficients (CV) of the analyzed samples are given in Table 2 (supplementary file). Likewise, average data of Post-Archean Australian shales (PAAS) and Upper Continental Crust (UCC) are presented in Table 2 supplementary file and used here in to represent average shale composition,

Major element distribution reflects the mineralogy of studied samples. As expected, calcareous shale samples are enriched in CaO. D300, 301, 302 samples in Derindere and C273, C274, C276 samples in Çeltikli core exhibit higher CaO concentrations. Compositional variations of Derindere and Çeltikli core samples are comparatively low, with the exception CaO values, in agreement with the mineralogical results (Table 2 supplementary file). The average concentrations of SiO_2, Al_2O_3, Fe_2O_3 and MgO concentrations in the Derindere core are 43.74 wt%, 20.04 wt%, 9.86 wt% and 2.53 wt% and 44 wt%, 18.30 wt%, 8.30 wt% and 2.80 wt% in the Çeltikli core. The vertical distribution of SiO_2, Al_2O_3, Fe_2O_3 and CaO elements are very similar in both cores (Table 2 supplementary file). Using the geochemical classification diagram of Herron (1988) all the samples are classified as shale except for a sample that falls in the wacke field (Figure 5). This is also supported by XRD data which indicate high clay ratios.

Major element data which is compatible with mineralogical data may be used to establish the element-mineral associations for shales. Although the element associations may change from one sample to another, a correlation analysis would demonstrate the general trends. Correlation graphics between major elements and Al_2O_3 are shown in Figure 6. With the exception of MgO, CaO, P_2O_5, SiO_2, Na_2O the major oxides show significant positive correlation with Al_2O_3 demonstrating that Al, K, Cr and Ti sources are mainly from feldspar and clay minerals as revealed from the XRD analysis (Figure 4). There is a significant positive correlation with LOI and CaO (r=0.96) in all samples suggesting that carbonates play an important role on the LOI of the shale samples (Figure 6). Rb displays strong positive correlation with K_2O (r=0.70) suggesting that both these elements are probably supplied by illite and muscovite components (Figure 6) (Plank and Langmuir, 1998). Bozkaya et al., (2009) pointed illite, illite/smectite (I-S) mixed layer clays and kaolinite minerals in Dadaş Formation.

Selected trace elements were compared with PAAS (Taylor and McLennan, 1985). The distributions of the elements in core shales are shown in Figure 7. Dadaş Shales have similar Cr, Rb, Y, Nb, Sc contents and show slightly depletion patterns in Ni, Cu Pb, Zr and Hf, slightly enrichment in Zn. Little differences of Cu, Ni and Zn contents with respect to PAAS can be attributed to chemical weathering diversity. Lower contents of Zr and Hf with respect to PAAS are associated with heavy minerals, such as zircon, which is resistant to weathering (Murali et al., 1983).

REE geochemistry

Concentrations of REE together with some elemental ratios are listed in Table 3 (supplementary file). REE show a strong positive correlation with the group of Al_2O_3, Fe_2O_3, Na_2O, K_2O, TiO_2, MnO and Cr_2O_3 and, and a negative correlation with MgO and CaO (Figure 8a).

Table 1. Whole-rock mineral percentages (%) of samples from Derindere drill hole (a) Celtikli drill hole (b) Maturity Index MMI = 100* [phyllosilicates/(phyllosilicates + quartz + feldspars)]. (Bathia, 1985).

DERINDERE CORE								CELTIKLI CORE							
Whole Rock Minerals (%)								Whole Rock Minerals (%)							
Sample							MMI	Sample							MMI
Number	Rock Name	Clay	Feldspar	Quartz	Calcite	Dolomite		Number	Rock Name	Clay	Feldspar	Quartz	Calcite	Dolomite	
D288	Shale	67.0	8.0	5.0	5.0	15.0	83.8	Shale	C263	55.0	18.0	12.0	4.0	11.0	64.7
D291	Shale	69.0	9.0	7.0	4.0	11.0	81.2	Shale	C265	63.0	7.0	7.0	2.0	21.0	81.8
D294	Shale	68.0	7.0	9.0	6.0	10.0	81.0	Shale	C266	54.0	15.0	10.0	7.0	14.0	68.4
D296	Shale	66.0	8.0	10.0	2.0	14.0	78.6	Shale	C267	57.0	14.0	9.0	5.0	15.0	71.3
D297	Shale	62.0	9.0	12.0	5.0	12.0	74.7	Shale	C269	55.0	15.0	8.0	5.0	17.0	70.5
D300	Carbonated shale	67.0	5.0	4.0	19.0	5.0	88.2	Shale	C271	67.0	12.0	11.0	4.0	6.0	74.4
D301	Carbonated shale	68.0	4.0	8.0	14.0	6.0	85.0	Carbonated shale	C273	58.0	10.0	7.0	20.0	5.0	77.3
D302	Carbonated shale	63.0	6.0	7.0	16.0	8.0	82.9	Carbonated shale	C274	56.0	8.0	9.0	18.0	9.0	76.7
d305	Shale	74.0	8.0	8.0	5.0	5.0	82.2	Carbonated shale	C276	62.0	7.0	8.0	19.0	4.0	80.5
D306	Shale	70.0	7.0	5.0	7.0	11.0	85.4	Shale	C279	65.0	9.0	8.0	10.0	8.0	79.3
Average		67.4	7.1	7.5	8.3	9.7	82.3		Average	59.2	11.5	8.9	9.4	11.0	74.5
St dev		3.2	1.6	2.3	5.5	3.4	3.6		St dev	4.4	3.7	1.6	6.6	5.3	5.3

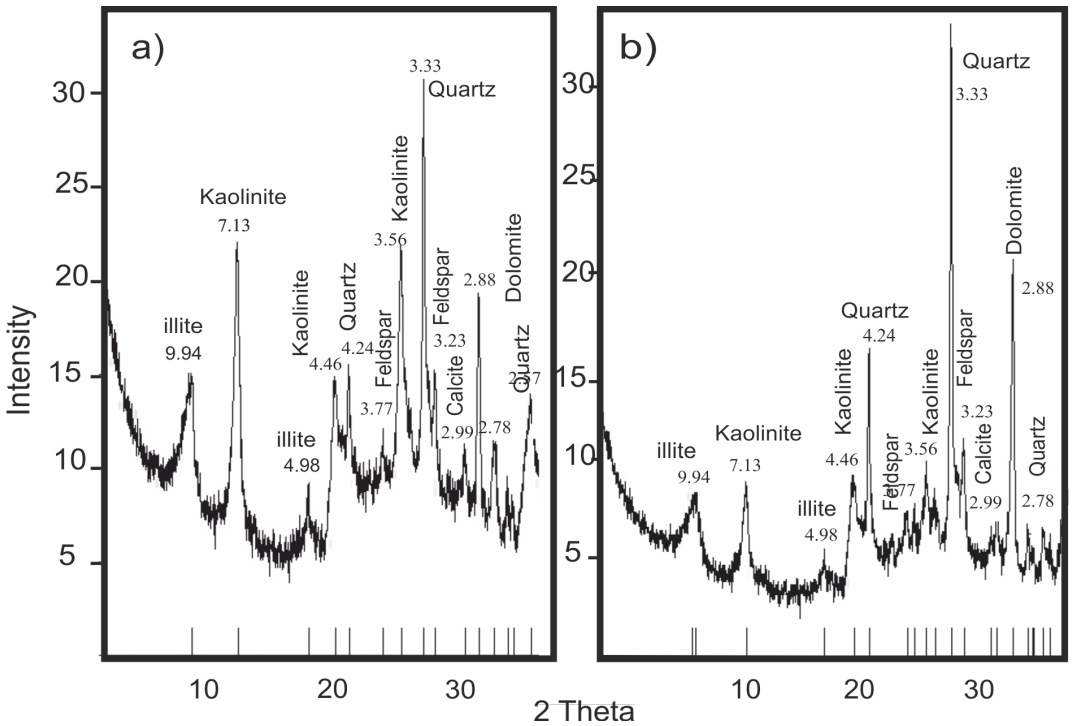

Figure 4. XRD pattern of sample no: a) D 266 from Derindere core, b) C 265 from Çeltikli core. The characteristic peak intensities (I, arrow) of minerals were normalized to that of the (104) reflection of dolomite for semiquantitative analyses of whole rock minerals according to Gündoğdu (1982) after Brindley (1980).

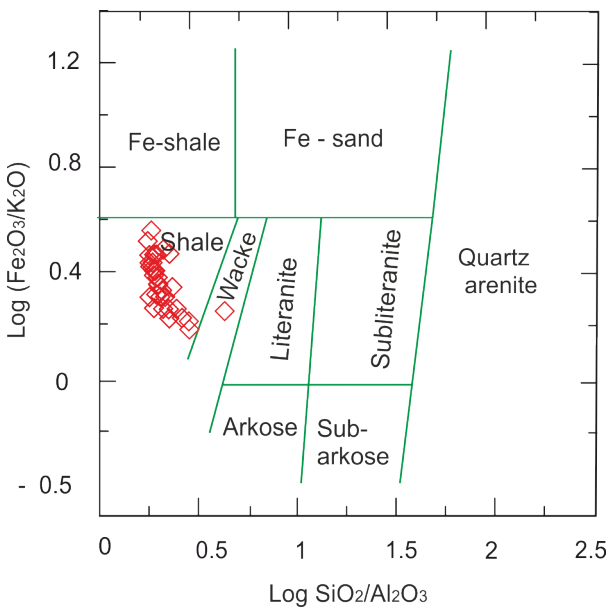

Figure 5. Log(Fe_2O_3/K_2O) vs log(SiO_2/Al_2O_3) of samples plotted on geochemical classification diagram after Herron (1988).

The correlation analysis has been used to find out the relationship of REE in rocks and their mineral components (Figure 8b). Total REEs are positively correlated with Co, Cs, Ga, Nb, Rb, Sn, Ta, Th, and Y which indicates that REEs are associated with clay minerals. The sorption of REE on clay minerals was reported by Milodowsky and Zalasiewich (1991) and Coppin et al. (2002). Total REEs are negatively correlated with Hf and Zr indicating that REEs are associated with clay minerals rather than zircon. The negative correlation of total REEs with U, Mo, Cu, Pb and Ni might be due to strong association of these elements with sulfur (Figure 8b). Effective role of sulfides in the REE concentration in black shale is discussed by Tait (1988).

Chondrite-normalized patterns of Dadaş samples, Bedinan Formation (from Tetiker, 2014) were compared with North American Shale Composite (NASC) and PAAS in Figure 9. The shale samples show LREE enrichment and flat HREE pattern with negative Eu anomaly and are similar to those of NASC and PAAS. In most of samples, Gd, Tb and Dy (HREE) concentrations are higher than PAAS. The relative depletion in the HREEs compared the LREEs may be due to a lower concentration of high REE-bearing heavy minerals such as zircon, rutile, sphene and garnet (Nyakairu and Koeberl, 2001). Lastly, Dadaş shale

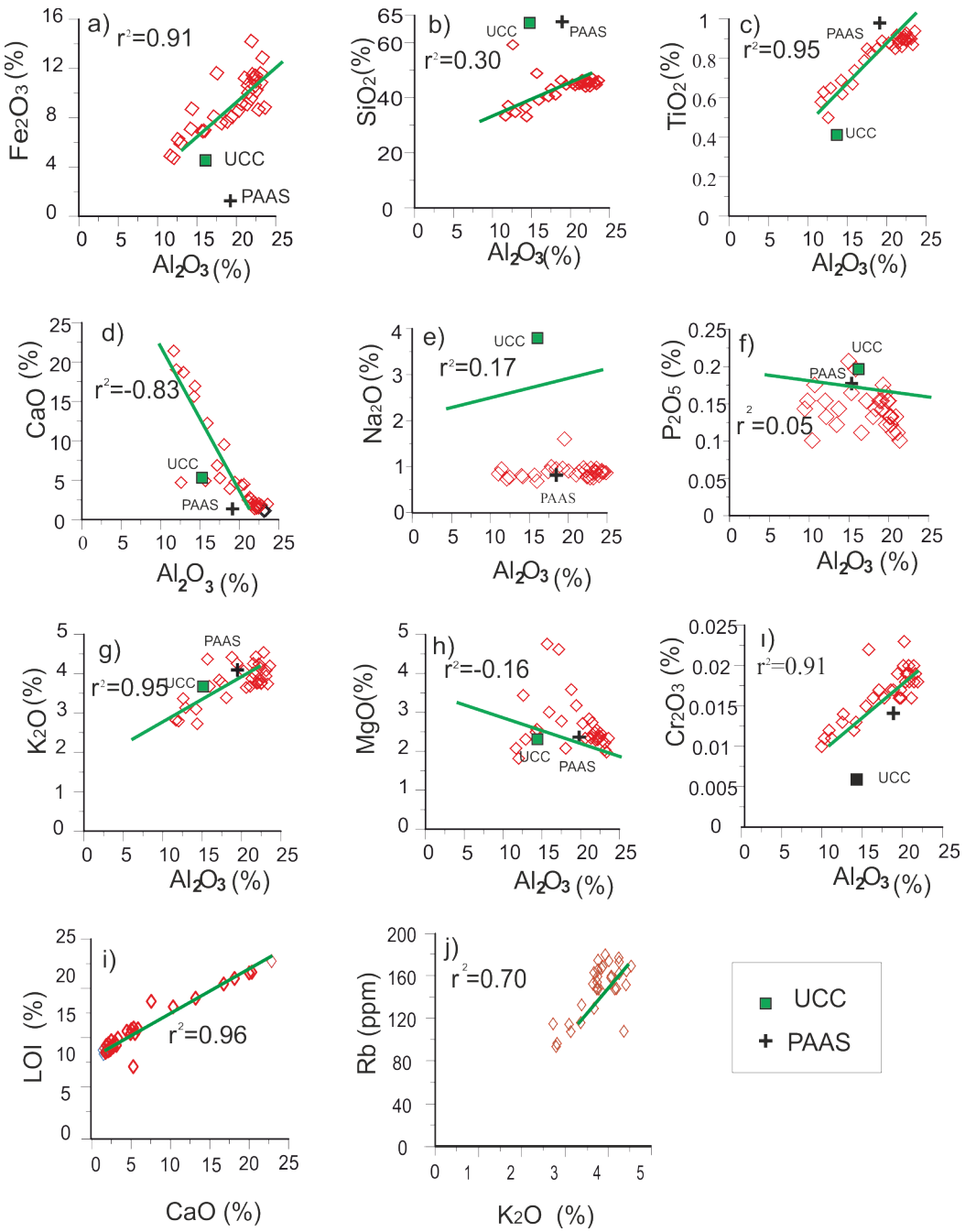

Figure 6. Correlation graphics between a-ı) major elements and Al_2O_3, average data of Upper Continental Crust (UCC) and PAAS, (data from Taylor and McLennan, 1985) also plotted for comparison, i-j) CaO and LOI, K_2O and Rb.

samples display significantly higher range of REE than Bedinan Formation.

The average shales have Ce/Ce* values of 1.0 (Cullers and Berendsen, 1998). Ce/Ce* values of studied samples are 0.83-0.96 that are consistent with average shale values (Table 3 supplementary file). This is also supported by geochemical classification diagram in Figure 5.

Organic matter sulfur contents and element relations

Total organic carbon (TOC), total carbon (TC) and total sulfur (TS) contents of Dadaş Shales are shown in Table 2 supplementary file. Averages of TOC, TC and TS values are 0.68%, 2.38%, 0.54% in the Derindere core and 0.64%, 2.80% and 0.60% in the Çeltikli core.

Organic material content is slightly high at depth of

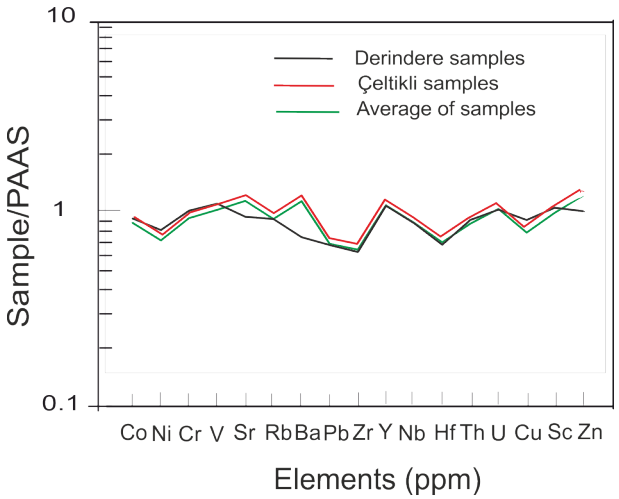

Figure 7. Average trace element contents of samples compared to average PAAS of Taylor and McLennan (1985).

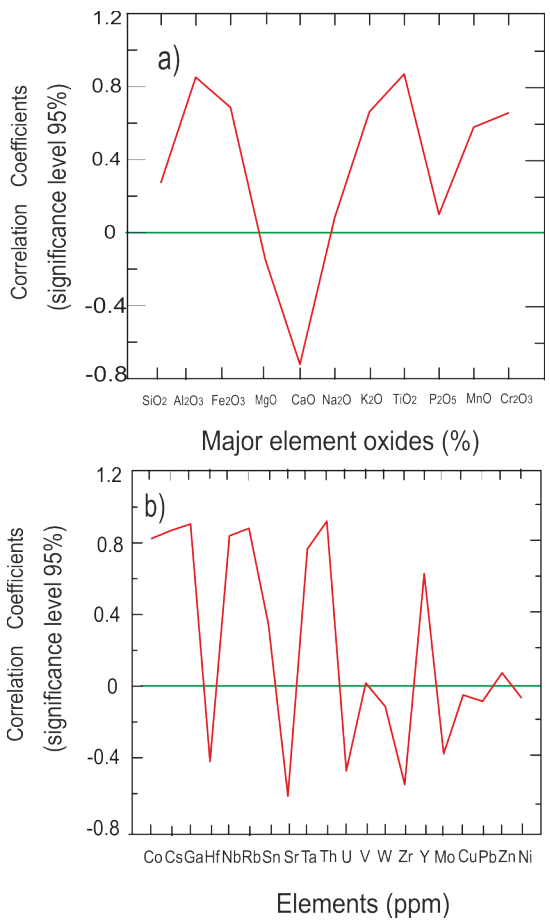

Figure 8. Correlation coefficients between a) total REE and major oxides b) total REE, and trace elements.

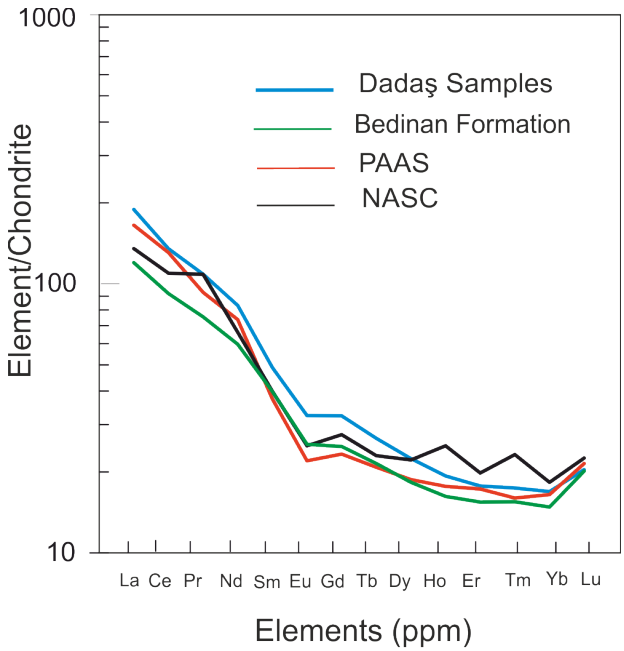

Figure 9. Chondrite-normalized (values from Sun and McDonough, 1989) REE patterns of Dadaş Samples, PAAS (data from Taylor and McLennan, 1985) and North American Shale Composite (data from Gromet et al., 1984) is also given as reference.

3000 to 3030 m in the Derindere core and 2730 to 2770 m in the Çeltikli core but significantly increases at depth of 3030 to 3070 m in the Derindere core and 2770 to 2790 m in the Çeltikli core (Table 2 supplementary file).

The positive correlations of TC with CaO might be indicative of the accumulation of Ca in carbonates (Table 2 supplementary file). Mo, Ni, As concentrations have a close relationship with organic material (Koralay and Sarı, 2013). TOC shows a positive correlation with these elements supporting this phenomenon (Table 4).

DISCUSSION

Paleoweathering and paleoclimate

Alkali and alkaline earth elements are useful in paleo-weathering studies because they are rapidly removed during weathering, and can be used to obtain the degree of chemical weathering around the source areas at the time of sedimentation (Nesbit and Young, 1984). Weathering of source area is one of the most important processes affecting the composition of sedimentary rocks. Chemical Index of Alteration (CIA) proposed by Nesbitt and Young (1984) is widely used used to investigate the degree of alteration. This index can be calculated using molecular proportions: $[Al_2O_3/(AI_2O_3+CaO^*+K_2O+Na_2O)\times100]$, where CaO* is the amount of CaO incorporated in the

Table 4. Correlation coefficients between some trace elements, REEs, TOC (%), TC (%) and total sulfur TS (%) contents of Dadaş Shales.

	SiO_2	Al_2O_3	CaO	P_2O_5	Mo	Cu	Pb	Zn	Ni	As
TOC	-0.13	-0.16	0.09	0.43	0.51	0.57	0.41	0.30	0.65	0.42
TC	-0.75	-0.85	0.90	0.48	0.46	0.21	0.13	0.12	0.35	0.49
TS	-0.3	-0.5	0.46	0.37	0.57	0.34	0.42	0.37	0.61	0.64

silicate fraction of the rock.

Generally, CIA values in Phanerozoic shales range from 70 to 75 which reflect a composition of muscovite, illite and smectite, and show a moderately weathered source, intensely weathered rocks yield mineral compositions trending toward kaolinite or gibbsite and a CIA approaching 100. CIA of unweathered rock is about 50. The Derindere and Çeltikli cores show CIA average of 75.17 and 72.42 which are consistent with moderate weathering (Table 2 supplementary file, Figure 10a). The Dadaş Shales are parallel to A-C line, showing leaching of CaO and Na_2O under moderate to intensive weathering processes from source rocks of the upper continental crust. In addition, they have relatively high Th/Sc and low Zr/Sc ratios suggesting negligible sediment recycling and sorting expressed by zircon enrichments (McLennan et al. 1993) (Tables 2; Figure 10b). This is in accordance with a generally immature "syntectonic" character of Dadaş Shales and is also reflected in mineralogy. According to Bozkaya et al. (2009), the Dadaş Formation contains quartz, feldspar, sericite, and muscovite. They conducted detailed clay analysis and indicated that the Silurian sedimentary units are illite, illite-smectite mixed layer clay (I-S), and kaolinite. They also stated that illite and I-S point to a muscovite-rich composition.

According to Leo et al. (2002), elemental variations are associated with paleoclimate-based sea level changes and changes in deposition conditions. The Dadaş Shales were deposited in a shelf environment and consequently variations in element concentrations reflect deposition conditions and paleoclimate. Zhao et al. (2007) used the C-value the ratio of ∑(Fe+Mn+Cr+Ni+V+Co)/∑(Ca+Mg +Sr+Ba+K+Na) to study the Permian paleoclimate of northwest China's Junggar Basin, and suggested that this ratio is between 0.2-0.8 for semiarid to semi-moist climates. The C-values of Dadaş Shales range from 0.18 to 1.66 (average 0.97 in Derindere core, 0.69 in Çeltikli core), reflecting a generally moist paleoclimate during early Paleozoic time (Table 2 supplementary file). According to Tolluoğlu and Sümer (1995), Gondwana

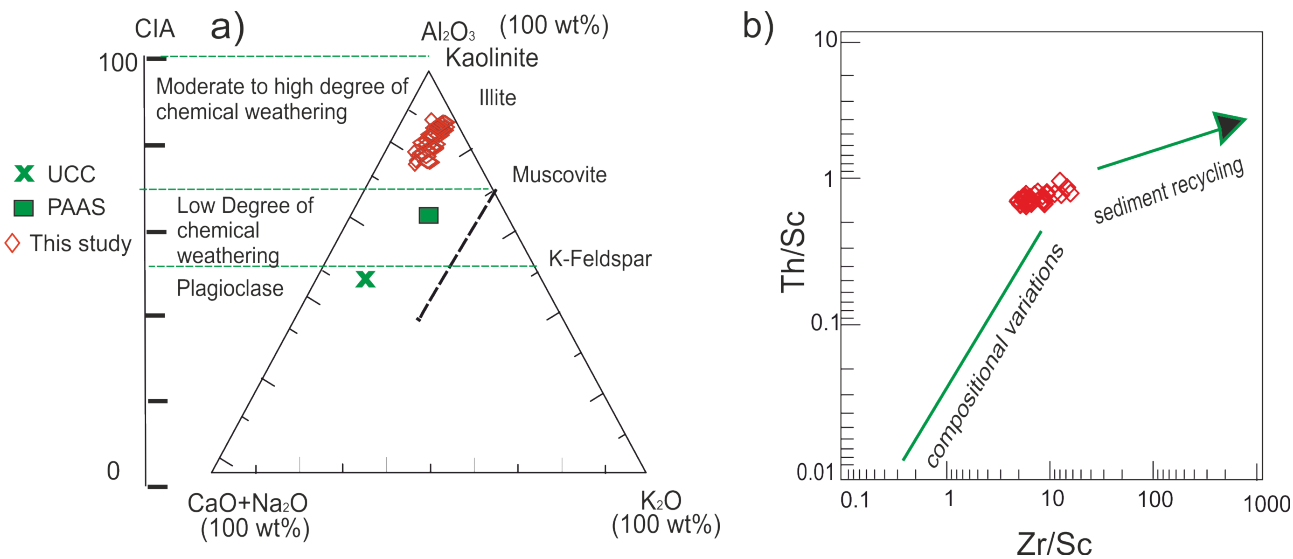

Figure 10. a) Al_2O_3-(CaO + Na_2O)-K_2O plot of sediment samples (after Nesbit and Young, 1984), compared data with PAAS and UCC given by Taylor and McLennan (1985), b) Th/Sc vs Zr/Sc diagram for Dadaş Shale (after McLennan et al., 1993) by the addition of average UCC (McLennan, 2001).

moved to South Pole in the Early Ordovician which resulted in invasion of Africa by glaciers. As a result of melting of continental glacier masses in Africa and South America the Early Silurian started with a rise in the sea level (Ziegler et al., 1977). Because of this partial transgression, organic material-rich dark shales and shale-alternated sandstone-carbonate units were deposited on top of glacial conglomerates. Likewise, Göncüoğlu and Turhan (1984) stated glacio-eustatic sea-level changes and formation of periglacial deposits during Late Ordovician-Early Silurian and rapid subsidence due to global sea-level rise and deposition of clastics during Mid-Late Silurian. In addition in both cores semiarid and semi-moist levels can be distinguished (Figure 11). C values and ∑ REE contents are decreased towards to arid regime. Tanaka et al. (2007) suggested that detrital materials predominantly control REE characteristics and higher REEs indicate higher detrital contribution to the marine environment due to excess precipitation in moisture climate. Calcite abundance is also increased with arid climate. Küçükuysal et al. (2013) showed that the increase in calcite in the Quaternary sediments in Turkey with the increasing aridity and the prevalence of the dry season. In arid climate, evaporation occurs and during the progressive evaporation of water the first precipitate is $CaCO_3$ (calcite) in most cases (Sinha and Raymahashay, 2009).

Paleoredox conditions

Ratios of several trace elements have been recommended for the evaluation of paleoredox conditions. Under reducing conditions, Co, Cr, Ni, V, and U are absorbed by the sediments. Ni/Co, V/Cr have been used to estimate the paleoredox conditions (Mir, 2015).

According to Jones and Manning (1994), Ni/Co ratios <5 suggest oxic conditions, 5-7 dysoxic conditions and >7 suboxic to anoxic conditions Cr exists only in detrital fraction and is not affected by redox conditions. Thus high V/Cr values are accepted to be an indicator of anoxic conditions (Dill, 1986). Jones and Manning (1994) also used V/Cr ratios of <2 to infer oxic conditions, 2-4.25 for dysoxic conditions and >4.25 suboxic to anoxic conditions. In addition, Ni/Co and V/Cr ratios of studied samples still suggest oxic-dysoxic conditions for the environment (Figure 12). U/Th and Cu/Zn ratios were also used to check redox conditions. Low U contents are generally found in sediments deposited in oxygenated conditions, high U contents are found in sediments from the oxygen minimum zone; for this reason, the U/Th ratio may be used as a redox indicator. U/Th ratios below 1.25 suggest oxic conditions for deposition, whereas values above 1.25 indicate suboxic and anoxic conditions. While low Cu/Zn values indicate oxidizing conditions, high Cu/Zn values show reducing conditions (Ramkumar et al., 2015; Mir, 2015). In the studied shales, low U/Th (average 0.28 in Derindere core, 0.30 in Çeltikli core) and Cu/Zn (average 0.56 in Derindere core, 0.43 in Çeltikli core) ratios suggest oxic conditions of deposition (Table 2 supplementary file).

In oxic conditions, Ce is less readily dissolved in

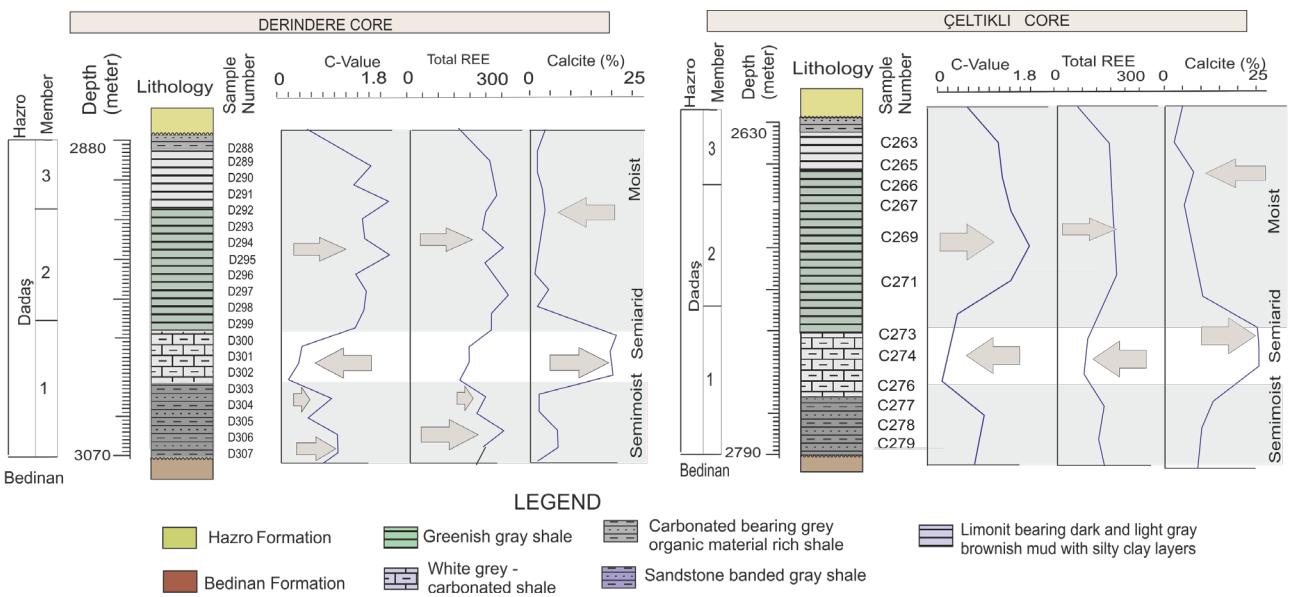

Figure 11. The relative contents of C-values, total rare earth elements (Σ REE) and calcite contents of Derindere and Çeltikli core samples. Arid to moisture paleoclimate was evaluated according to C-value=ratio of (Fe+Mn+Cr+Ni+V+Co)/(Ca+Mg+Sr+Ba+K+Na), after Zhao et al., 2007.

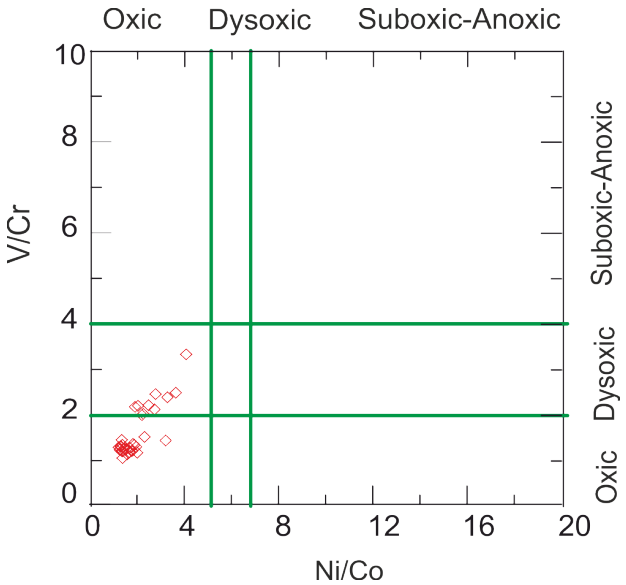

Figure 12. Ni/Co vs V/Cr plot of samples (after Rimmer et al., 2004).

seawater, which shows negative Ce anomaly (Elderfield and Greaves, 1982). Oxic sediments on the other hand are more enhanced with respect to Ce and show less negative to positive Ce anomaly (>-0.1) (Wright et al., 1987; Chen et al., 2012). Ce anomaly values of Dadaş shales are between -0.01 and 0.23 indicating that shales were deposited under oxic to weakly oxic conditions (Table 3 supplementary file).

TOC contents of samples are very low which also reflect the oxic-dioxic character of the depositional environment. According to Tribovillard et al. (2006), sediments under oxic-dysoxic conditions have TOC contents of <2%. As shown from Table 4a, TOC contents of most samples are <2%.

Provenance

Shales generally reflect provenance of siliciclastic sediments due to their homogeneity and post depositional impermeability. The geochemical compositions of terrigenous sediments are frequently used by many researchers to infer the provenance, because they tend to reflect source rock composition. Provenance studies are common for sedimentary rocks (Al-Juboury and Al-Hadidy, 2009; Armstrong-Altrin, 2009; Armstrong-Altrin et al., 2015 a,b; Garzanti et al., 2016). To characterize the provenance of shales, it is necessary to rely on elements that are the least mobile during weathering, transport, diagenesis and metamorphism (Wronkiewicz and Condie, 1990).

Major oxides, such as TiO_2 and Al_2O_3, are generally used for provenance interpretations. A discriminating criterion has been applied to distinguish different types of parent igneous rocks, with Al_2O_3/TiO_2 ratios of 3-8 for mafic igneous rocks, 8-21 for intermediate igneous rocks, and 21-70 for felsic igneous rocks. The average Al_2O_3/TiO_2 ratio is 23.73 in Derindere core and 22. 80 in Çeltikli core (Table 2 supplementary file) suggest felsic- intermediate igneous rock compositions for samples. The provenance discrimination diagram of Roser and Korsch (1988) has been widely used in recent studies to discriminate the provenance of clastic sediments (Castillo et al., 2015). On this diagram, most of Dadaş Shale samples show intermediate, basic composition except for 2 samples that plot inside the felsic and quartz sedimentary provenance field, respectively (Figure 13a). As a whole, most core sediments were derived from rocks of intermediate composition varying between felsic and mafic rock types.

The REEs, Y, Zr, Th, Sc, Hf, and Co are valuable elements for examining the source-area composition (Taylor and McLennan, 1985; McLennan and Taylor, 1991). These elements have very short residence times in the water column. In addition, some element ratios are useful for distinguishing felsic from mafic source components in shales (Taylor and McLennan, 1985; Wronkiewicz and Condie, 1990; Cullers, 1994). It is shown in Figure13b that La/Sc, Th/Sc, Th/U, Rb/Sr, La/Ni, Cr/Th, Zr/Sc, Zr/Th, Zr/Hf, $(La/Yb)_N$ (N, chondrite normalized values from Sun and McDonough, 1989) ratios of Dadaş Shales have similar composition to those of UCC and PAAS except for Zr/Sc ve Zr/Th ratios. Element ratios of mafic and felsic source rocks such as La/Sc, Sc/Th, Cr/Th, Co/Th and Eu/Eu* differ significantly and hence provide useful information on the provenance of sedimentary rocks (Cullers and Podkovyrov, 2000). When these ratios are compared, composition of Dadaş Shales is compatible with sediments derived from felsic rocks, the upper continental crust (UCC), and PAAS (Table 5). On the other hand higher values of Sc/Th, Cr/Th, Co/Th in Dadaş Shales with respect to sands from silicic rocks may indicate the presence of relatively higher proportion of basic material in their source. This is shown in the La/Th vs Hf provenance discrimination diagram of Floyd and Leveridge (1987) (Figure 13c). In the graphic Dadaş Shales are scattered near to the mixed felsic/basic source fields. Tetiker (2014) studied geochemistry of Bedinan Formation and concluded that sandstones represent a range of magmatic provenance regions, mostly from quartz sedimentary to partially felsic and mafic composition. Ordovician glaciers formed from these lithologies and melted in Silurian possibly provided source material for the Dadaş Formation.

The REE patterns are also used to infer sources of sedimentary rocks, since basic rocks contain low LREE/HREE ratios and no Eu anomalies, whereas more silicic

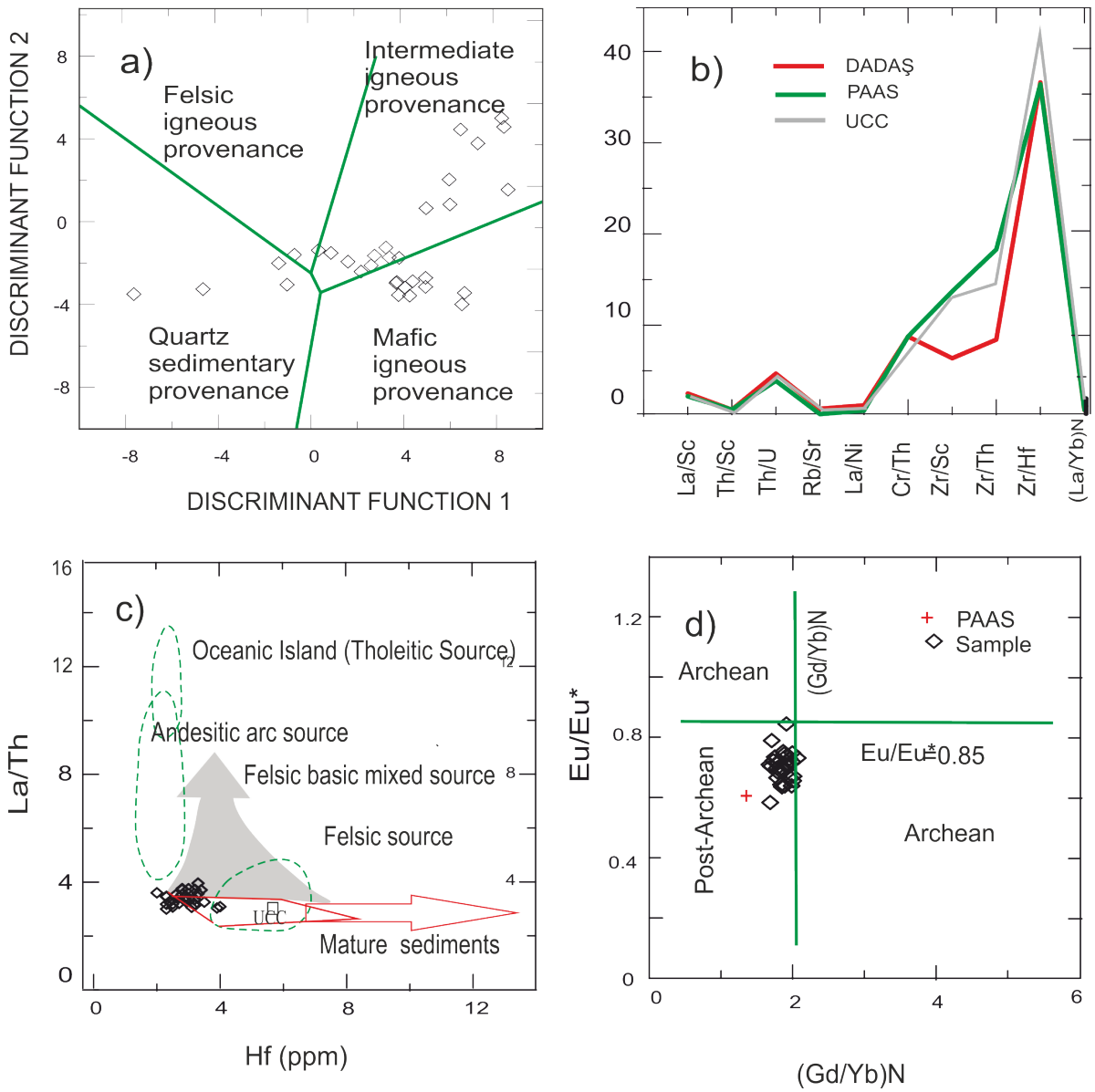

Figure 13. a) Discriminant function diagram of samples show provenance (Roser and Korsch, 1988). The discriminant functions are: Discriminant Function 1 = (-1.773·TiO_2)+(0.607·Al_2O_3)+(0.760·Fe_2O_3)+(-1.500·MgO)+(0.616·CaO)+(0.509·Na_2O)+(-1.224·K_2O)+(-9.090); Discriminant Function 2 = (0.445·TiO_2)+(0.070·Al_2O_3)+(-0.250·Fe_2O_3)+(-1.142·MgO)+(0.438·CaO)+(1.475·Na_2O)+(1.426·K_2O)+(-6.861), b) spider diagram of some elemental ratios of provenance for samples (For PAAS, data from Gromet et al., 1984 and for UCC Taylor and Mclennan, 1985), c) La (ppm)/Th (ppm) vs Hf (ppm) diagram indicating the composition of sedimentary rocks as a function of source rock derivation, d) Eu/Eu* vs $(Gd/Yb)_N$ (N, chondrite normalized values from Sun and McDonough, 1989) diagrams for samples.

rocks usually contain higher LREE/HREE ratios and negative Eu anomalies (Cullers, 1994). Regarding the Dadaş Shales, fractionated REE patterns $(La/Yb)_N$ are between 8,57-12.77 and $(Gd/Yb)_N$ are between 1.68 and 2.07 (N=chondrite normalized to values of Sun and McDonough, 1989).These values are compatible with UCC and PAAS (Table 3 supplementary file). In the Eu/Eu* vs $(Gd/Yb)_N$ graphic, the samples overlap each other and plot well within the field that depict the PAAS source (Figure 13d).

Tectonic setting

Major and trace-elements and their various bivariate and multivariate plots with discrimination functions are

Table 5. Comparison of core samples and element ratios in range of sediments from felsic and mafic rocks (data from Cullers and Podkovyrov, 2000), UCC and PAAS (data from Taylor and McLennan, 1985).

Elemental ratio	Dadaş samples		Range of sediments		UCC	PAAS
	Derindere	Çeltikli	Felsic rocks	Mafic rocks		
Th/Sc	0.73	0.74	0.84-20.5	0.05-0.22	0.79	0.90
Th/Co	0.61	0.62	0.67-19.4	0.04-1.4	0.63	0.63
Cr/Th	8.74	8.36	4.0-15.0	25-500	7.76	7.53
La/Sc	2.46	2.62	2.5-16.3	0.43-0.86	2.21	2.40

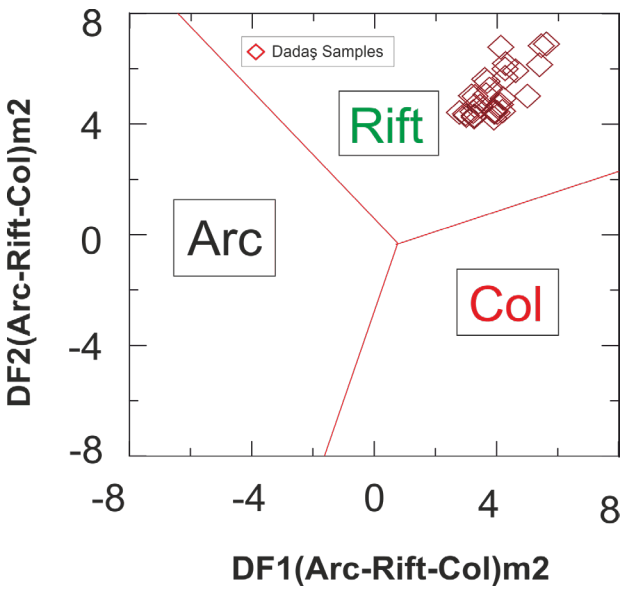

Figure 14. Discriminant-function multi-dimensional diagram for low-silica clastic sediments (Verma and Armstrong-Altrin, 2013). The subscript $_{m2}$ in DF1 and DF2 represents the low-silica diagram based on log_e-ratio of major elements. Discriminant function equations are:
$DF1(Arc\text{-}Rift\text{-}Col)_{m2}=(0.608xIn(TiO_2/SiO_2)adj)+(-1.854\cdot In(Al_2O_3/SiO_2)adj)+(0.299\cdot In(Fe_2O_3{}^tSiO_2)adj)+(-0.550\cdot In(MnO/SiO_2)adj)+(0.120\cdot In(MgO/SiO_2)adj)+(0.194\cdot In(CaO/SiO_2)adj)+(-1.510\cdot In(Na_2O/SiO_2)adj)+(1.941\cdot In(K_2O/SiO_2)adj)+(0.003\cdot In(P_2O_5/SiO_2)adj)-0.294$
$DF2(Arc\text{-}Rift\text{-}Col)_{m2}=(-0.554\cdot In(TiO_2/SiO_2)adj)+(-0.995\cdot In(Al_2O_3/SiO_2)adj)+(1.765\cdot In(Fe_2O_3{}^t/SiO_2)adj)+(-1.391\cdot In(MnO/SiO_2)adj)+(-1.034\cdot In(MgO/SiO_2)adj)+(0.225\cdot In(CaO/SiO_2)adj)+(0.713\cdot In(Na_2O/SiO_2)adj)+(0.330\cdot In(K_2O/SiO_2)adj)+(0.637\cdot In(P_2O_5/SiO_2)adj)-3.631.$

mostly applicable for tectonic setting of the sedimentary basins. Various diagrams are available to identify the tectonic setting of a source region (e.g. Murray, 1992; Bhatia, 1983; Bhatia and Crook, 1986; Roser and Korsch, 1986). These diagrams were evaluated by other researchers (e.g. Armstrong-Altrin and Verma, 2005; Verma and Armstrong-Altrin, 2016). Verma and Armstrong-Altrin (2013) proposed two new discriminant-function-based major-element diagrams for the tectonic discrimination of siliciclastic sediments from three main tectonic settings; island or continental arc, continental rift and collision have been created for the tectonic discrimination of high-silica (SiO_2)adj=63-95% and low-silica rocks (SiO_2)adj=35-63% (the adj values are adjusted to 100% on an anhydrous basis).These diagrams were successfull used in recent studies to discriminate the tectonic setting of a source region (Armstrong-Altrin et al., 2014; Armstrong-Altrin, 2015). SiO_2 of Dadaş samples are low silica rocks (SiO_2 values are between 33.10-59.29%). According to low-silica diagrams Dadaş sediments are plotted within the rift field (Figure 14). During the Early Paleozoic time, there was a rifting in the southeastern Anatolia.

Ruban et al. (2007) suggested that in Paleozoic time the Middle East terranes were affected by the evolution of the Paleozoic Tethyan oceans, the Hun and Cimmerian superterranes, and the Gondwana and Pangaea supercontinents. They also suggested that at least three major Paleozoic rift episodes occurred along the margins of Gondwana and Pangea. The first was in the Early Ordovician when Avalonia broke off from Gondwana. At the Latest Ordovician-Earliest Silurian times glaciers advanced over regions of Gondwana reaching western Saudi Arabia (Figure 15 a,b).The second involved the Mid-Silurian breakaway of the Hun Superterrane (Figure 15c). Following the glaciations in the Gondwana in Ordovician, Toridia uplift (420 Ma) is reported to be another important event in southeastern Anatolia (Tolluoğlu and Sümer, 1995). Tolluoğlu and Sümer (1995) mention migmatite

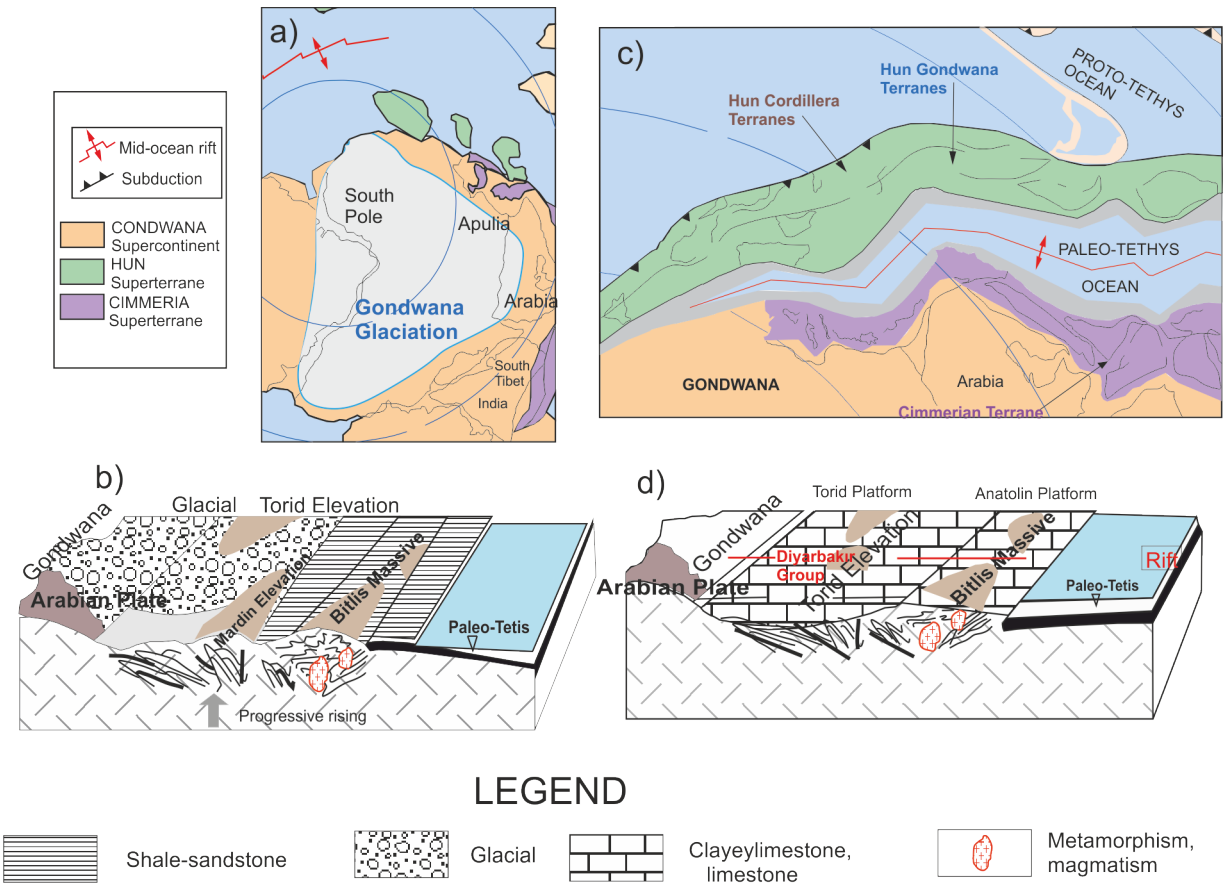

Figure 15. a) Plate-tectonic reconstruction of the Latest Ordovician-Earliest Silurian times glaciers advanced over regions of Gondwana reaching western Saudi Arabia (from Ruban et al., 2007), b) the Middle-Late Silurian shows the Hun Superterrane rifting away from the Gondwana Supercontinent (from Ruban et al., 2007), c) Early Silurian glacial conglomerates (modified from Tolluoğlu and Sümer, 1995), d) Middle Silurian-Early Devonian transgression and continental rift formation (modified from Tolluoğlu and Sümer, 1995).

formation and anatexis granites via deformation and uplift of Anatolia microcontinent and Taurides. This continental rift formation gave rise to deposition of sediments of Diyarbakır Group which corresponds to Dadaş Shales of felsic to neutral composition accompanied by Bedinan Formation (Figure 15d). This proposed rifting in southeastern Anatolia was first revealed in this study by diagrams of Verma and Armstrong-Altrin (2013).

CONCLUSIONS

The chemical composition of the analysed sediments is controlled by source-area composition, weathering, paleoredox, paleoclimate and tectonic setting.

CIA values of Dadaş samples are consistent with medium weathering. The C-values shows mainly moist climatic conditions influenced the Dadaş Shales at Early Silurian-Early Devonian time. Ni/Co, V/Cr, U/Th, Cu/Zn, Ce/Ce* values suggest the oxic depositional environment which is also in support of low TOC values of samples.

Geochemical data indicate magmatic and partly sedimentary provenance for Dadaş Shale. The geochemical characteristics preserve the signatures of sediments derived from UCC. Fe_2O_3/TiO_2, $Al_2O_3/(Al_2O_3+Fe_2O_3+MnO)$, Th/U, Rb/Sr, La/Ni, Cr/Th, Eu/Eu* ratios of shales are similar to UCC and PAAS composition.

Higher LREE/HREE ratios and negative Eu anomalies, fractionated REE patterns with $(La/Yb)_N$, $(Gd/Yb)_N$ values are similar to PAAS and characteristic of sediments derived from the UCC. But the higher values of Sc/Th, Cr/Th, Co/Th in Dadaş Shales with respect to sands from silicic rocks may indicate the presence of relatively higher proportion of basic material in their source. This is also supported by provenance discrimination and La/Th vs Hf diagram. It is possible that mafic components were derived from undermost Ordovician Bedinan Formation which is supported by the fact that Bedinan Formation

contains not only felsic but also basic components.

As conclusion, thickening of continental crust and continental rifting in the region triggered by oceanic rifting in Ordovician exerted a major control in composition of Ordovician Bedinan Formation. Following transgression in Silurian supplied source material to Dadaş Formation from underlying lithologies. A second rifting was developed in the Middle Silurian and migmatite and anatexis events in the upper crust affected the composition of Dadaş Formation which is revealed by the presence of components with variable compositions in the sediments. This rifting in southeastern Anatolia was revealed by new discriminant-function-based major-element diagrams for the tectonic discrimination of siliciclastic sediments. Petrographic and stratigraphic data on Dadaş Formation presented in previous studies have been supported first time by geochemical findings in the present study. On a regional scale, the equivalents of Paleozoic Dadaş Shales are widespread and geochemical study of these marine sediments can be used to add new insights into the Paleozoic stratigraphic evolution.

ACKNOWLEDGEMENTS

The financial support of the Fırat University (Turkey) Scientific Research Projects Unit under FUBAP-MF.11.09 project number is gratefully acknowledged. We would like to thank Turkish Petroleum Corporation (TPAO), ACME (Canada) and General Directorate of Mineral Research and Exploration (Ankara, Turkey) for chemical and mineralogical analysis. We are grateful to the editor and anonymous reviewers whose helpful reviews have greatly improved the manuscript.

REFERENCES

Al-Juboury A.I. and Al-Hadidy A.H., 2009. Petrology and depositional evolution of the Paleozoic rocks of Iraq. Marine and Petroleum Geology 26, 208-231.

Armstrong-Altrin J.S. and Verma S.P., 2005. Critical evaluation of six tectonic setting discrimination diagrams using geochemical data of Neogene sediments from known tectonic settings. Sedimentary Geology 177, 115-129.

Armstrong-Altrin J.S., 2009. Provenance of Sands from Cazones, Acapulco, and Bahía Kino Beaches, Mexico, Revista Mexicana de Ciencias Geológicas 26, 764-782.

Armstrong-Altrin J.S., Nagarajan R., Madhavaraju J., Rosalez-Hoz L., Lee Y.I, Balaram V., Cruz-Martínez A., Avila-Ramírez G., 2013. Geochemistry of the Jurassic and Upper Cretaceous shales from the Molango Region, Hidalgo, eastern Mexico: Implications for source-area weathering, provenance, and tectonic setting. Comptes Rendus Geoscience 345, 185-202.

Armstrong-Altrin J.S., Nagarajan R., Lee Y.I., Zubillaga J.J.K., Saldana L.P.C., 2014. Geochemistry of sands along the San Nicolas and San Carlos beaches, Gulf of California, Mexico: implications for provenance and tectonic setting. Turkish Jornal of Earth Sciences 23, 533-558.

Armstrong-Altrin J.S., Machain-Castillo M.L., Rosales-Hoz L., Carranza-Edwards A., Sanchez-Cabeza J.A., Ruíz-Fernández A.C., 2015a. Provenance and depositional history of continental slope sediments in the Southwestern Gulf of Mexico unraveled by geochemical analysis. Continental Shelf Research 95, 15-26.

Armstrong-Altrin J.S., Nagarajan R., Balaram V., Natalhy-Pineda O., 2015b. Petrography and geochemistry of sands from the Chachalacas and Veracruz beach areas, western Gulf of Mexico, Mexico: constraints on provenance and tectonic setting. Journal of South American Earth Sciences 64,199-216.

Armstrong-Altrin J.S., 2015. Evaluation of two multidimensional discrimination diagrams from beach and deep-sea sediments from the Gulf of Mexico and their application to Precambrian clastic sedimentary rocks. International Geology Review 57, 1446-1461.

Aydemir A., 2012. Comparison of Mississippian Barnett Shale, northern-central Texas, USA and Silurian Dadas Formation in southeast Turkey. Journal of Petroleum Science and Engineering 80, 81-93.

Bauluz B., Mayayo M.J., Fernandez-Nieto C., Lopez J.M.G., 2000. Geochemistry of Precambrian and Paleozoic siliciclastic rocks from the Iberian Range (NE Spain): implications for source-area weathering, sorting, provenance, and tectonic setting. Clays and Clay Minerals 48, 374-384.

Bhatia M.R., 1983. Plate tectonics and geochemical composition of sandstones. Journal of Geology 91, 611-627.

Bhatia M.R., 1985. Rare earth element geochemistry of Australian Paleozoic greywackes and mudrocks: provenance and tectonic control. Sedimentary Geology 45, 97-113.

Bhatia M.R. and Crook A.W., 1986. Trace element characteristics of greywackes and tectonic setting discrimination of sedimentary basins. Contributions to Mineralogy and Petrology 92, 181-193.

Bozdoğan N., Bayçelebi O., Willink R., 1987. Paleozoic stratigraphy and petroleum potential of the Hazro area, S.E. Turkey. The 7th Biannual Petroleum Congress of Turkey, Ankara (Turkey), 117-130.

Bozkaya Ö., Yalçın H., Kozlu H., 2009. The mineralogy of Paleozoic rocks from the Amanos region. Hacettepe University Bulletin for Earth Sciences 30, 11-44.

Brindley G.W., 1980. Quantitative X-ray Mineral Analysis of Clays. Crystal Structures of Clay Minerals and Their X-ray Identification. Mineralogical Society, London, 411-438.

Castillo P., Lacassie J.P., Augustsson C., Herve F., 2015. Petrography and geochemistry of the Carboniferous Triassic Trinity Peninsula Group, West Antarctica: implications for provenance and tectonic setting. Geological Magazine 152, 575-588.

Chen L., Lin A.T.S., Xuejuan D., Haisheng Y., Luis Loung-Yie T., Guiwen X., 2012. Level changes recorded by cerium

anomalies in the Late Jurassic (Tithonian) Black Rock Series of Qiangtang Basin, north-central Tibet. Oil Shale 29, 18-35.

Coppin F., Berger G., Bauer A., Castet S., Loubet M., 2002. Sorption of lanthanides on smectite and kaolinite. Chemical Geology 182, 57-68.

Cullers R.L., 1994. The controls on the major and trace element variation of shales, siltstones, and sandstones of Pennsylvanian-Permian age from uplifted continental blocks in Colorado to platform sediment in Kansas, (USA). Geochimica Cosmochimica Acta 58, 4955-4972.

Cullers R.L. and Berendsen P., 1998. The provenance and chemical variation of sandstones associated with the Mid-Continent Rift system, USA. European Journal of Mineralogy 10, 987-1002.

Cullers R.L., 2000. The geochemistry of shales, siltstones and sandstones of Pennsylvanian - Permian age, Colorado, U.S.A.: implications for provenance and metamorphic studies. Lithos 51, 181-203.

Cullers R.L. and Podkovyrov V.M., 2000. Geochemistry of the Mesoproterozoic Lakhanda shales in southeastern Yakutia, Russia: Implications for mineralogical and provenanace, and recyling. Precambrian Research 104, 77-93.

Dill H., 1986. Metallogenesis of Early Paleozoic graptolite shales from the Graefenthal Horst northern Bavaria-Federal Republic of Germany. Economic Geology 81, 889-903.

Elderfield H. and Greaves M.J., 1982. The rare earth elements in seawater. Nature 296, 214-219.

Floyd P.A. and Leveridge B.E., 1987. Tectonic environment of the Devonian Gramscatho basin, south Cornwall: framework mode and geochemical evidence from turbiditic sandstones. Journal of the Geological Society of London 144, 531-542.

Garzanti E., Al-Juboury A.İ., Zoleikhaei Y., Vermeesch P., Jotheri J., Akkoca D.B., Kadhim Obaid A., Mark B.A., Andó S., Limonta M., Padoan M., Resentini A., Rittner M., Vezzol G., 2016. The Euphrates-Tigris-Karun river system: Provenance, recycling and dispersal of quartz-poor foreland-basin sediments in arid climate. Earth-Science Reviews 162, 107-128.

Göncüoğlu M.C. and Turhan N., 1984. Geology of the Bitlis metamorphic belt. In: Geology of the Taurus Belt. (Eds.): O. Tekeli and M.C. Göncüoğlu, Proceedings of the International Symposium on the Geology of the Taurus Belt, Ankara (Turkey), 237-244.

Gromet L.P., Dymek R.F., Haskin L.A., Korotev R.L., 1984. The North American shale composite: its compilation, major and trace element characteristics. Geochimica et Cosmochimica Acta 48, 2469-3482.

Gündoğdu M.N., 1982. Geological, mineralogical and geochemical investigation of Neogene Bigadiç Basin. PhD thesis, Hacettepe University, Ankara, Turkey, 368 pp. (in Turkish).

Herron M.M., 1988. Geochemical classification of terrigenous sands and shales from core or log data. Journal of Sedimentary Petrology 58, 820-825.

Iztan Y.H., 2004. GDA X ve XI Bolgeler Paleozoik Birimlerinin (Dadas, Bedinan) Jeokimyasal Degerlendirilmesi. TPAO Report No: 4539,Ankara,85 pp. (in Turkish).

Jones B. and Manning D.A.C., 1994. Comparison of geological indices used for the interpretation of palaeoredox conditions in ancient mudstones. Chemical Geology 111, 111-129.

Kavak O. and Toprak S., 2013. Organic geochemıcal and petrographic properties of Hazro Dadaş (Diyarbakır) coals. Bulletin of the Mineral Research and Exploration Bulletin of MTA 147, 91-113.

Khanehbad M., Moussavi-Harami R., Mahboubi A., Nadjafi M., Mahmudy Gharaie M.H., 2012. Geochemistry of Carboniferous sandstones (Sardar Formation), East-Central Iran: implication for provenance and tectonic setting. Acta Geologica Sinica 86, 1200-1210.

Kozlu H. and Göncüoğlu M.C., 1997. Stratigraphy of the Infracambrian Rock-units in the Eastern Taurides and their correlation with similar units in southern Turkey. Turkish Associate Petrol Geol Special Publication 3, 50-61.

Koralay D.B. and Sarı A., 2013. Redox conditions and metal-organic carbon relations of Eocene bituminous shales (Veliler/Mengen-Bolu/Turkey). Energy Sources 17, 1597-1607.

Küçükuysal C., Türkmenoğlu A.G., Kapur S., 2013. Multi-proxy evidence of Mid-Pleistocene dry climates observed in calcretes in Central Turkey. Turkish Journal of Earth Sciences 22, 463-483.

Lee Y., 2002. Provenance derived from the geochemistry of the Palaeozoic-early Mesozoic mudrocks of the Pyeongan Supergroup, Korea. Sedimentary Geology 149, 219-235.

Leo D.P., Dinelli E., Mongelli G., Schiattarella M., 2002. Geology and geochemistry of Jurassic pelagic sediments, Scisti silicei Formation, southern Apennines, Italy. Sedimentary Geology 150, 229-246.

Maden Tetkik ve Arama Genel Müdürlüğü (MTA), 2002. 1: 500000 ölçekli Türkiye Jeoloji Haritaları, Diyarbakır paftası, MTA Genel Müdürlüğü, Ankara.

McCarroll D., 2016. Simple Statistical Tests for Geography. Taylor and Francis Group, 334 pp.

McLennan S.M. and Taylor S.R., 1991. Sedimentary rocks and crustal evolution-tectonic setting and secular trends. Journal of Geology 99, 1-21.

McLennan S.M., Hemming S., McDaniel D.K., Hanson G.N., 1993. Geochemical approaches to sedimentation, provenance, and tectonics. Processes Controlling the Composition of Clastic Sediments. Geological Society of America, Special Paper 284, 21-40.

McLennan, 2001. Relationships between the trace element composition of sedimentary rocks and upper continental crust. Geochemistry Geophysics Geosystems 2,1-24.

Milodowsky A.E. and Zalasiewicz J.A., 1991. Redistribution of rare-earth elements during diagenesis of turbidite/hemipelagite mudrock sequences of Llandovery age from central Wales.

Geological Society London Special Publications 57, 101-124.

Mir A.R., 2015. Rare earth element geochemistry of Post- to Neo-Archean shales from Singhbhum mobile belt, Eastern India: implications for tectonic setting and paleo-oxidation conditions Chinese Journal of Geochemistry 34, 401-409.

Murali A.V., Parthasarathy R., Mahadevan T.M., Sankar D. M., 1983. Trace element characteristics, REE patterns and partition coefficients of zircons from different geological environments - a case study on Indian zircons: Geochimica et Cosmochimica Acta 47, 2047-2052.

Murray R.W., Bucholtzten Brink M.R., Gerlach D.C., Russ G.P., Jones D.L., 1992. Interoceanic variations in the rare earth, major and trace element depositional chemistry of chert: perspectives gained from the DSDP and ODP record. Geochimica Cosmochiica Acta 56, 1897-1913.

Nesbitt H.W. and Young G.M., 1984. Prediction of some weathering trends of plutonic and volcanic rocks based on thermodynamic and kinetic considerations. Geochimica. Cosmochimica Acta 48, 1523-1534.

Nyakairu G.W.A. and Koeberl C., 2001. Mineralogical and chemical composition and distribution of rare earth elements in clay-rich sediments from central Uganda. Geochemical Journal 35, 13-28.

Özdemir F. and Ünlügenç Ü.C., 2013. Evaluation of hydrocarbon potential and stratigraphy of Gokici (Diyarbakır) structure. Cukurova University Journal of the Faculty of Engineering and Architecture 1, 127-141.

Perinçek D., Duran O., Bozdoğan N., Çoruh T., 1991. Stratigraphy and paleo-geographical evolution of the autochthonous sedimentary rocks in the SE Turkey. Ozan Sungurlu Symposium, Ankara, (Turkey), 274-305.

Plank T. and Langmuir C.H., 1998. The chemical composition of subducting sediment and its consequences for the crust and mantle. Chemical Geology 145, 325-394.

Ramkumar M., Kumaraswamy K., Mohanraj R., 2015. Environmental Management of River Basin Ecosystems. Heidelberg, Springer Verlag, 761 pp.

Rimmer S.M., Thompson J.A., Goodnight S.A., Robl T., 2004. Multiple controls on the preservation of organic matter in Devonian-Mississippian marine black shales: geochemical and petrographic evidence. Palaeogeography, Palaeoecology, Palaeoclimatology 215 (3), 125-154.

Roser B.P. and Korsch R.J., 1986. Determination of tectonic setting of sandstone mudstone suites using SiO_2 content and K_2O/Na_2O ratio. The Journal of Geology 94, 635-10.

Roser B.P. and Korsch R.J., 1988. Provenance signatures of sandstone-mudstone suites determined using discriminant function analysis of major-element data. Chemical Geology 67, 119-139.

Ruban D.A., Moujahed I., Al-Husseini M.I, Iwasaki. Y., 2007. Review of Middle East Paleozoic plate tectonics. GeoArabia 12, 35-56.

Sun S.S. and McDonough W.F., 1989. Chemical and isotopic systematics of oceanic basalts; implications for mantle composition and processes. In: Magmatism in the Ocean Basins. (Eds.): A.D. Saunders and M.J. Norry, Geological Society of London, London, 313-345.

Sinha R. and Raymahashay R., 2009. Salinity model inferred from two shallow cores at Sambhar salt lake Rajasthan. Journal of Geological Society of India 56, 213-217.

Stolle E., Yalcin M.N., Kavak O., 2011. The Permian Kas Formation of SE Turkey-palynological correlation with strata from Saudi Arabia land Oman. Geological Journal 46, 561-573.

Tait S.R., 1988. Samples from the crystallizing boundary layer of a zoned magma chamber. Contributions to Mineralogy and Petrology 100, 470-483.

Tanaka K., Akagawa F., Yamamoto K., Tani Y., Kawabe I., Kawai T., 2007. Rare earth element geochemistry of Lake Baikal sediment: its implication for geochemical response to climate change during the Last Glacial/Interglacial transition. Quaternary Science Reviews 26, 1362-1368.

Tawfik H.A., Ghandour I.M., Maejima W., Armstrong-Altrin J.S,. Abdel-Monem T.A., 2017. Petrography and geochemistry of the siliciclastic Araba Formation (Cambrian), east Sinai, Egypt: implications for provenance, tectonic setting and source weathering. Geological Magazine 1-23.

Taylor S.R. and McLennan S.H., 1985. The geochemical evaluation of the continental crust.Reviews in Geophysics 33, 241-265.

Tetiker S., 2014. Petrography and geochemistry of early Palaeozoic clastic rocks from the southeast Anatolian autochthone rocks in Mardin area (Derik-Kızıltepe), Turkey. Carpathian Journal of Earth and Environmental Sciences 1, 149-162.

Tolluoğlu A.Ü. and Sümer E.Ö., 1995. An evolutionary model on Early Paleozoic of Anatolian microcontinent, northern margin of Gondwana Land. Geological Bulletin of Turkey 38, 2, 1-22.

Tribovillard N., Algeo T.J., Lyons T., Riboulleau A., 2006. Trace metals as paleoredox and paleoproductivity proxies: An update. Chemical Geology 232, 12-32.

Verma S.P., Armstrong-Altrin J.S., 2013. New multi-dimensional diagrams for tectonic discrimination of siliciclastic sediments and their application to Precambrian basins. Chemical Geology 355, 117-133.

Verma S.P., Díaz-González L., Armstrong-Altrin J.S., 2016. Application of a new computer program for tectonic discrimination of Cambrian to Holocene clastic sediments. Earth Science Informatics 9, 151-165.

Verma S.P. and Armstrong-Altrin J.S., 2016. Geochemical discrimination of siliciclastic sediments from active and passive margin settings. Sedimentary Geology 332, 1-12.

Wright J., Schrader H., Holster W.T., 1987. Paleoredox variations in ancient oceans recorded by rare earth elements in fossil apatite. Geochimica et Cosmochimica Acta 51, 631-644.

Wronkiewicz D.J. and Condie K.C., 1990. Geochemistry and mineralogy of sediments from the ventersdorp and transvaal supergroups, South Africa: Cratonic evolution during the early Proterozoic. Geochimica Cosmochimica Acta 54, 343-354.

Zhao Z.Y., Zhao J.H., Wang H.J., Liao J.D., Liu C.M., 2007. Distribution characteristics and applications of trace elements in Junggar Basin. Natural.Gas Exporation and Develoment 30, 30-33.

Ziegler A.M., Hansen K.S., Johnson M.E., Kelly M.A., Scotese C.R., Von Der Voo R., 1977. Silurian Continental distributions, paleogeography, climatology and biogeography. Tectonophysics 40, 13-51.